Mechanism and Machine Theory 130 (2018) 330–345

Contents lists available at ScienceDirect

Mechanism and Machine Theory

journal homepage: www.elsevier.com/locate/mechmachtheory

A homogeneous payload specific performance index for robot manipulators based on the kinetic energy

S. Nader Nabavi[a], Alireza Akbarzadeh[a,*], Javad Enferadi[b], Iman Kardan[a]

[a] Mechanical Engineering Department, Center of Excellence on Soft Computing and Intelligent Information Processing (SCIIP), Ferdowsi University of Mashhad, Mashhad, Iran
[b] Mechanical Engineering Department, Mashhad Branch, Islamic Azad University, Mashhad, Iran

ARTICLE INFO

Article history:
Received 9 February 2018
Revised 19 June 2018
Accepted 7 August 2018
Available online 6 September 2018

Keywords:
Dexterity
Kinetic energy index
Kinetic energy ellipsoid
Homogeneous performance index

ABSTRACT

Performance indices are extensively used in the optimization of robot structures. However, in the case of manipulators with mixed translational and rotational DOFs, traditional indices are not readily applicable due to the non-homogeneity of the Jacobian matrix. In this paper, special cases of generalized inertia ellipsoid, GIE, [1] and rms velocity norm [2] are used to define a payload specific performance index based on the transferred kinetic energy to the payload. The proposed kinetic energy index, KEI, is dimensionally homogeneous and is independent from the units. Moreover, this index is scale invariant and simultaneously considers both of the translational and rotational motions. A unit KEI indicates that a uniform kinetic energy is transferred to the payload for all the feasible joint velocities. For better representations, kinetic energy ellipsoids are drawn using a new vector form definition of the kinetic energy. A two-link manipulator and a 3-RRR robot are considered as case studies for evaluation of the proposed index. The kinetic energy ellipsoids and contours of KEI value are plotted over the entire workspace of the two robots. For a given payload with specified dynamic characteristics, KEI can be used to design an optimal structure of the manipulator such that a uniform kinetic energy is transferred to the payload.

1. Introduction

An important step in designing a manipulator is to optimize its geometrical and structural parameters. In order to evaluate the performance of the robots, multiple indices have been introduced such as the condition number, manipulability, dexterity, structural length, accuracy, stiffness, etc [3–5].

The dexterity index measures the maneuverability of the manipulators in positioning and orienting their end-effector, EE. This index is extensively used in the design and optimization of different manipulators. A small dexterity value indicates that the robot is in a singular configuration. In this configuration the robot does not have the ability to deal with external forces in certain directions and its maneuverability is decreased [6]. To ensure that the robot is not in a singular configuration, the condition number of its Jacobian matrix is examined in different configurations. The Jacobian matrix maps the robot velocities between joint space and Cartesian space. If the rank of the Jacobian matrix is reduced in a certain position, that configuration is said to be singular.

* Corresponding author.
E-mail address: ali_akbarzadeh@um.ac.ir (A. Akbarzadeh).

https://doi.org/10.1016/j.mechmachtheory.2018.08.007
0094-114X/

Nowadays, researchers apply multiple performance indices to determine certain structures and configurations where the robot is in good manipulability conditions. The most popular indices are based on the manipulability concept [7] and dexterity criteria [8], proposed to enhance the maneuverability of manipulators. In many studies, the condition number of the Jacobian matrix is used as a kinematic accuracy index [9–11]. Using the condition number of the Jacobian matrix, the error amplification factor is investigated between the joint space and Cartesian space of the robots. In [12,13] the concepts of the manipulability and dexterity are interpreted based on the manipulability ellipsoids which depend on the manipulator Jacobian. When the manipulability ellipsoid is close to a sphere, the robot is in a good maneuverability condition.

Most of the available indices suffer from the non-homogeneity issue, occurring when the manipulators have mixed translational and rotational degrees of freedom, DOF. This issue causes the indices to provide inaccurate and unreliable performance measures. Specifically, measuring the condition number of a non-homogeneous Jacobian matrix is physically meaningless [14].

Researchers have proposed different methods for resolving the non-homogeneity issue of the Jacobian matrix. Instead of considering the translational and rotational velocities of the EE, Gosselin [15] used a Jacobian matrix between the joint velocities and the linear velocities of two specific points on the EE. Pond and Carretero [16] extended the Gosselin idea and presented a dimensionally homogeneous Jacobian matrix between the joint velocities and the linear velocities of three points on the moving platform. However, this method may result in different Jacobian matrices because of some arbitrariness in selection of the points on the EE. Some references propose to use a characteristic length of the robot as a scaling factor to homogenize the Jacobian matrix [17–20]. The arrays of the Jacobian matrix with length dimension are divided by the chosen characteristic length. Various methods are proposed for defining a suitable characteristic length, each of which may result in a different scaling factor and consequently a different value for the performance indices. Another method for homogenizing the Jacobian matrix is to separate the translational and rotational motions of the EE [21–23]. Using this method, two homogeneous Jacobian matrices are obtained for translational and rotational motions of the EE, each of which should be studied separately. Clearly, one aspect of the robot motions, translational or rotational, is ignored in this method. Moreover, separate optimization of the translational and rotational parts does not guarantee a well-conditioned overall Jacobian matrix.

The concept of generalized inertia ellipsoid, GIE, represents the dynamic isotropy of a manipulator. When GIE becomes a sphere, the manipulator is in a dynamic isotropy configuration and the nonlinear dynamic forces are reduced [1]. GIE is defined based on the kinetic energy of the whole manipulator. Therefore, this concept can be used to define a homogenous performance index which considers the translational and rotational movements simultaneously. In this paper, a special case of GIE concept and rms velocity norm [2] are used to define a payload specific kinetic energy index, KEI, for performance evaluation of manipulators. Instead of considering the kinetic energy of the whole manipulator, the proposed index merely measures the transferred kinetic energy to the payload. This index is particularly useful in some applications, e.g. motion simulators, where the robot should be design to move a given payload or when the mass and inertia of the robot components are negligible comparing to the payload. In fact, for a given payload with specified dynamic characteristics, KEI may be applied to find an optimized structure of manipulator in which a uniform kinetic energy is transferred to the payload for all the feasible joint velocities.

Besides its clear physical interpretation, the proposed kinetic energy index, resolves the non-homogeneity issue and considers both the translational and rotational motions of the manipulator, simultaneously. In this paper, the behavior of the new index is studied for the cases of a serial manipulator and a parallel robot. The kinetic energy ellipsoids are plotted over the entire workspace of the robots as well as the contours of their KEI value. The kinetic energy ellipsoids are defined based on a new vector form definition of the kinetic energy of the payload.

The rest of this paper is organized as follows. In Section 2 the new vector form of the kinetic energy is defined for a general manipulator. Section 3 introduces the KEI index and defines the concept of the kinetic energy ellipsoids. The proposed index is evaluated through implementation on a two link serial manipulator and a 3-$\underline{R}$RR parallel robot as the two case studies in Section 4. This section also compares the behavior of the KEI with some well-known performance indices for the two selected robots. Finally, Section 5 concludes the paper.

2. Kinetic energy of the payload

This paper seeks to define a payload specific performance index which is dimensionally homogeneous and considers both of the translational and rotational motions of robots. The rms velocity norm proposed by Lin et al. [2] provides a very good tool for this purpose. The rms norm is given by,

$$\left\| {}^{\mathcal{B}}\mathbf{t}_P \right\|_{rms} = \left({}^{\mathcal{B}}\mathbf{t}_P^T \mathbb{R}\mathbb{M}\mathbb{R}^T {}^{\mathcal{B}}\mathbf{t}_P \right)^{1/2} \tag{1}$$

where,$\{\mathcal{B}\}$ is the base coordinate system and ${}^{\mathcal{B}}\mathrm{t}_P = [{}^{\mathcal{B}}\mathrm{V}_P^{\mathrm{T}},\ {}^{\mathcal{B}}\Omega_P^{\mathrm{T}}]^{\mathrm{T}}$ is the vector of the generalized velocity of the payload or, in other words, the twist vector of the payload. Moreover,

$$\mathbb{R} = diag\left({}^{\mathcal{B}}_{\mathcal{P}}\mathcal{R}, {}^{\mathcal{B}}_{\mathcal{P}}\mathcal{R}\right), \quad \mathbb{M} = \int \nu\left({}^{\mathcal{P}}\mathbf{r}\right) \begin{pmatrix} \mathbf{I} & {}^{\mathcal{P}}\hat{\mathbf{r}}^T \\ {}^{\mathcal{P}}\hat{\mathbf{r}} & -{}^{\mathcal{P}}\hat{\mathbf{r}}^2 \end{pmatrix} d\mathbf{r} \tag{2}$$

in which,$\{\mathcal{P}\}$ is a coordinate system attached to the payload, ${}^{\mathcal{B}}_{\mathcal{P}}\mathcal{R}$ is the rotation matrix from $\{\mathcal{P}\}$ to $\{\mathcal{B}\}$, $\nu({}^{\mathcal{P}}\mathrm{r})$ is a non-negative weighting function, $\mathbf{I}$ is the identity matrix, ${}^{\mathcal{P}}\mathrm{r}$ is the position vector of elements on the EE and ${}^{\mathcal{P}}\hat{\mathrm{r}}$ is the skew-symmetric matrix of the vector ${}^{\mathcal{P}}\mathrm{r}$.

In this paper, a special case of the rms velocity norm is used where ν is the mass density. In this case the rms norm simplifies to the kinetic energy of the payload on the EE. In order to gain a better physical sense, the rms norm is re-driven based on the definition of the kinetic energy of the payload in the following.

In a general form, the kinetic energy of the payload is obtained as,

$$\mathcal{K}_P = \frac{1}{2}M_P\mathbf{V}_P\cdot\mathbf{V}_P + \frac{1}{2}\boldsymbol{\Omega}_P^T\mathbf{I}_P\boldsymbol{\Omega}_P \tag{3}$$

where, M_P is the mass of the payload and $\mathbf{I}_P$ is its inertia tensor. $\mathbf{V}_P$ and $\boldsymbol{\Omega}_P$ are the vectors of the linear and angular velocities of the payload, respectively. The components of the velocity vectors and the inertia tensor can be defined in any arbitrary coordinate system, CS. Assuming that the coordinate system $\{\mathcal{P}\}$ is located at the center of mass of the payload and its axes are aligned with the principle axes, ${}^{\mathcal{P}}\mathbf{I}_P = diag({}^{\mathcal{P}}I_{P,11},\ {}^{\mathcal{P}}I_{P,22},{}^{\mathcal{P}}I_{P,33})$ will have a diagonal form. ${}^{\mathcal{P}}I_{P,ii}$ is the mass moment of inertia of the payload, calculated about the i^{th} axis of the coordinate system $\{\mathcal{P}\}$. Let ${}^{\mathcal{P}}\mathbf{V}_P = [{}^{\mathcal{P}}V_{P,1},{}^{\mathcal{P}}V_{P,2},{}^{\mathcal{P}}V_{P,3}]^T$ and ${}^{\mathcal{P}}\boldsymbol{\Omega}_P = [{}^{\mathcal{P}}\Omega_{P,1},{}^{\mathcal{P}}\Omega_{P,2},{}^{\mathcal{P}}\Omega_{P,3}]^T$ be the vectors of the linear and angular velocities of the payload whose components are expressed in the coordinate system $\{\mathcal{P}\}$. Therefore, the kinetic energy of the payload can be rewritten as,

$$\begin{aligned}\mathcal{K}_P = {} & \frac{1}{2}M_P\left({}^{\mathcal{P}}V_{P,1}^2+{}^{\mathcal{P}}V_{P,2}^2+{}^{\mathcal{P}}V_{P,3}^2\right)\\ & +\frac{1}{2}\left({}^{\mathcal{P}}I_{P,11}{}^{\mathcal{P}}\Omega_{P,1}^2+{}^{\mathcal{P}}I_{P,22}{}^{\mathcal{P}}\Omega_{P,2}^2+{}^{\mathcal{P}}I_{P,33}{}^{\mathcal{P}}\Omega_{P,3}^2\right)\end{aligned} \tag{4}$$

Clearly, the kinetic energy is a scalar quantity. However, for providing better visual representations, vector forms are more suitable for defining the performance indices [24,25]. Let the vector of oriented translational kinetic energy of the payload, ${}^{\mathcal{P}}_{T}\mathbf{k}_P$, and the vector of oriented rotational kinetic energy of the payload, ${}^{\mathcal{P}}_{T}\mathbf{k}_P$, be defined as,

$${}^{\mathcal{P}}_{T}\mathbf{k}_P = \begin{bmatrix}\frac{1}{\sqrt{2}}\sqrt{M_P}{}^{\mathcal{P}}V_{P,1}\\ \frac{1}{\sqrt{2}}\sqrt{M_P}{}^{\mathcal{P}}V_{P,2}\\ \frac{1}{\sqrt{2}}\sqrt{M_P}{}^{\mathcal{P}}V_{P,3}\end{bmatrix} = \frac{1}{\sqrt{2}}M_P^{0.5}{}^{\mathcal{P}}\mathbf{V}_P, \tag{5}$$

$${}^{\mathcal{P}}_{R}\mathbf{k}_P = \begin{bmatrix}\frac{1}{\sqrt{2}}\sqrt{{}^{\mathcal{P}}I_{P,11}}{}^{\mathcal{P}}\Omega_{P,1}\\ \frac{1}{\sqrt{2}}\sqrt{{}^{\mathcal{P}}I_{P,22}}{}^{\mathcal{P}}\Omega_{P,2}\\ \frac{1}{\sqrt{2}}\sqrt{{}^{\mathcal{P}}I_{P,33}}{}^{\mathcal{P}}\Omega_{P,3}\end{bmatrix} = \frac{1}{\sqrt{2}}{}^{\mathcal{P}}\mathbf{I}_P^{0.5}{}^{\mathcal{P}}\boldsymbol{\Omega}_P \tag{6}$$

in which, the matrix ${}^{\mathcal{P}}\mathbf{I}_P^{0.5}$ is defined as,

$${}^{\mathcal{P}}\mathbf{I}_P^{0.5} = diag\left(\sqrt{{}^{\mathcal{P}}I_{P,11}},\sqrt{{}^{\mathcal{P}}I_{P,22}},\sqrt{{}^{\mathcal{P}}I_{P,33}}\right) \tag{7}$$

Then the total oriented kinetic energy of the payload can be defined as,

$${}^{\mathcal{P}}\mathbf{k}_P = \begin{bmatrix}{}^{\mathcal{P}}_{T}\mathbf{k}_P\\ {}^{\mathcal{P}}_{R}\mathbf{k}_P\end{bmatrix} = \frac{1}{\sqrt{2}}\begin{bmatrix}M_P^{0.5}\mathbf{I}_{3\times3} & 0_{3\times3}\\ 0_{3\times3} & {}^{\mathcal{P}}\mathbf{I}_P^{0.5}\end{bmatrix}{}^{\mathcal{P}}\mathbf{t}_P \tag{8}$$

where, ${}^{\mathcal{P}}\mathbf{t}_P = [{}^{\mathcal{P}}\mathbf{V}_P^T,\ {}^{\mathcal{P}}\Omega_P^T]^T$ is the vector of the generalized velocity of the payload or, in other words, the twist vector of the payload. Therefore, the kinetic energy of the payload can be rewritten as,

$$\mathcal{K}_P = {}^{\mathcal{P}}\mathbf{k}_P\cdot{}^{\mathcal{P}}\mathbf{k}_P = {}^{\mathcal{P}}\mathbf{k}_P^T{}^{\mathcal{P}}\mathbf{k}_P \tag{9}$$

Using the concept of Jacobian matrices, the twist vector of the payload can be written as a function of the actuated joint velocities as,

$${}^{\mathcal{P}}\mathbf{t}_P = {}^{\mathcal{P}}\mathbf{J}_P\dot{\mathbf{q}} \tag{10}$$

where, $\dot{\mathbf{q}}$ is the velocity vector of the actuated joints and ${}^{\mathcal{P}}\mathbf{J}_P$ is the Jacobian matrix which maps $\dot{\mathbf{q}}$ to the generalized velocity vector of the payload in the CS $\{\mathcal{P}\}$. Separating the translational and rotational velocities of the payload, ${}^{\mathcal{P}}\mathbf{J}_P$ can be partitioned as,

$${}^{\mathcal{P}}\mathbf{t}_P = \begin{bmatrix}{}^{\mathcal{P}}\mathbf{V}_P\\ {}^{\mathcal{P}}\boldsymbol{\Omega}_P\end{bmatrix} = \begin{bmatrix}{}^{\mathcal{P}}_{T}\mathbf{J}_P\\ {}^{\mathcal{P}}_{R}\mathbf{J}_P\end{bmatrix}\dot{\mathbf{q}} \tag{11}$$

Using the partitioned Jacobian matrix, the total oriented kinetic energy of the payload can be re-written as,

$${}^{\mathcal{P}}\mathbf{k}_P = \frac{1}{\sqrt{2}}\begin{bmatrix}M_P^{0.5}{}^{\mathcal{P}}_{T}\mathbf{J}_P\\ {}^{\mathcal{P}}\mathbf{I}_P^{0.5}{}^{\mathcal{P}}_{R}\mathbf{J}_P\end{bmatrix}\dot{\mathbf{q}} = {}^{\mathcal{P}}\mathbf{E}\dot{\mathbf{q}} \tag{12}$$

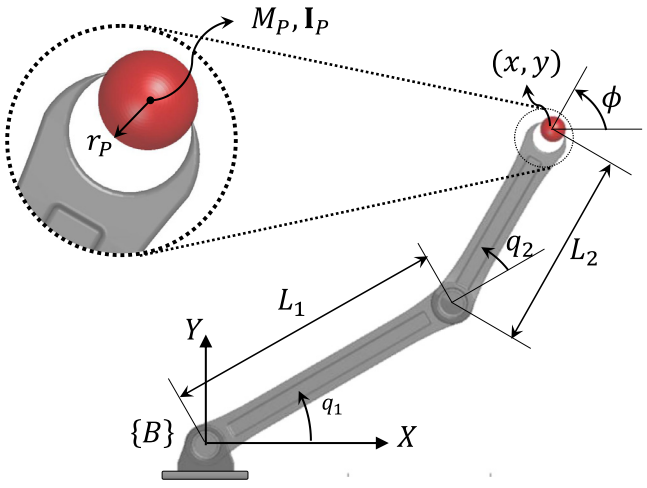

Fig. 1. Two DOF serial planar manipulator.

Finally, the kinetic energy of the payload is calculated as,

$$\mathcal{K}_P = \dot{\mathbf{q}}^T \left(\frac{1}{2} M_P {}^{\mathcal{P}}_{T}\mathbf{J}_P^T {}^{\mathcal{P}}_{T}\mathbf{J}_P + \frac{1}{2} {}^{\mathcal{P}}_{R}\mathbf{J}_P^T {}^{\mathcal{P}}\mathbf{I}_P {}^{\mathcal{P}}_{R}\mathbf{J}_P \right) \dot{\mathbf{q}} = \dot{\mathbf{q}}^T \mathcal{K} \dot{\mathbf{q}} \tag{13}$$

Clearly, the matrix $\mathcal{K}$ is a symmetric matrix and consequently, $\mathcal{K}_P$ is a quadratic form.
As proposed by Asada [1], the generalized inertia matrix, $\mathbf{I}_G$, of a manipulator is defined as,

$$\mathbf{I}_G = \frac{\partial^2 \mathcal{K}_M}{\partial \dot{\mathbf{q}}^2} \tag{14}$$

where, $\mathcal{K}_M$ is the total energy of the whole manipulator. It is easy to verify that, if in Eq. (14) $\mathcal{K}_M$ is replaced by $\mathcal{K}_P$, i.e. merely considering the kinetic energy of the payload, $\mathbf{I}_G$ simplifies to $\mathcal{K}$. Therefore, KEI is a special case of GIE concept.
Considering Eq. (11), $\mathcal{K}_P$ can be re-written as,

$$\mathcal{K}_P = \frac{1}{2} \left({}^{\mathcal{P}}\mathbf{t}_P^T \begin{bmatrix} M_P \mathbf{I} & 0 \\ 0 & {}^{\mathcal{P}}\mathbf{I}_P \end{bmatrix} {}^{\mathcal{P}}\mathbf{t}_P \right) \tag{15}$$

Meanwhile, ${}^{\mathcal{P}}\mathbf{t}_P = {}^{\mathcal{B}}_{\mathcal{P}}\mathcal{R}^T {}^{\mathcal{B}}\mathbf{t}_P$. Therefore, $\mathcal{K}_P = \frac{1}{2} \| {}^{\mathcal{B}}\mathbf{t}_P \|^2_{rms}$ in which,

$$\mathbb{M} = \begin{bmatrix} M_P \mathbf{I} & 0 \\ 0 & {}^{\mathcal{P}}\mathbf{I}_P \end{bmatrix} \tag{16}$$

3. Kinetic energy ellipsoids

Assuming the normality of the joint velocity vector, $\dot{\mathbf{q}}^{\mathrm{T}} \dot{\mathbf{q}} = 1$, the maximum kinetic energy of the payload can be found by defining the cost function $\mathbb{F}(\dot{\mathbf{q}})$ as,

$$\mathbb{F}(\dot{\mathbf{q}}) = \mathcal{K}_P - \Lambda \left(\dot{\mathbf{q}}^{\mathrm{T}} \dot{\mathbf{q}} - 1 \right) = \dot{\mathbf{q}}^{\mathrm{T}} \mathcal{K} \dot{\mathbf{q}} - \Lambda \left(\dot{\mathbf{q}}^{\mathrm{T}} \dot{\mathbf{q}} - 1 \right) = \dot{\mathbf{q}}^{\mathrm{T}} (\mathcal{K} - \Lambda \mathbf{I}) \dot{\mathbf{q}} + \Lambda \tag{17}$$

where, Λ is the Lagrange multiplier. Zeroing the partial derivative of $\mathbb{F}(\dot{\mathbf{q}})$ with respect to $\dot{\mathbf{q}}$ gives,

$$(\mathcal{K} - \Lambda^* \mathbf{I}) \dot{\mathbf{q}}^* = 0 \tag{18}$$

Eq. (18) is an eigenvalue equation. Therefore, the calculated Λ^*s are the eigenvalues of the matrix $\mathcal{K}$ and $\dot{\mathbf{q}}^*$ vectors are the corresponding joint space eigenvectors.
The matrix $\mathcal{K}_{\mathrm{n}\times\mathrm{n}}$ is a symmetric positive semi-definite matrix and consequently all of its eigenvalues are positive. In other words, $\Lambda^*_{\mathrm{i}} \geq 0$ for $i = 1, \ldots, n$ where n represents the dimension of the square matrix $\mathcal{K}$.
Clearly, the results of Eq. (18) correspond to the extreme values of $\mathcal{K}_P$ subjected to the normality constraint. Rewriting the Eq. (18) as $\mathcal{K}\dot{\mathbf{q}}^* = \Lambda^* \dot{\mathbf{q}}^*$ and substituting in Eq. (13) gives,

$$\mathcal{K}_P = \dot{\mathbf{q}}^{*\mathrm{T}} \mathcal{K} \dot{\mathbf{q}}^* = \Lambda^* \dot{\mathbf{q}}^{*\mathrm{T}} \dot{\mathbf{q}}^* = \Lambda^* \tag{19}$$

Therefore, the maximum eigenvalue, Λ^*_{max}, equals the maximum kinetic energy transferred to the payload and the minimum eigenvalue, Λ^*_{min}, equals the minimum kinetic energy of the payload.

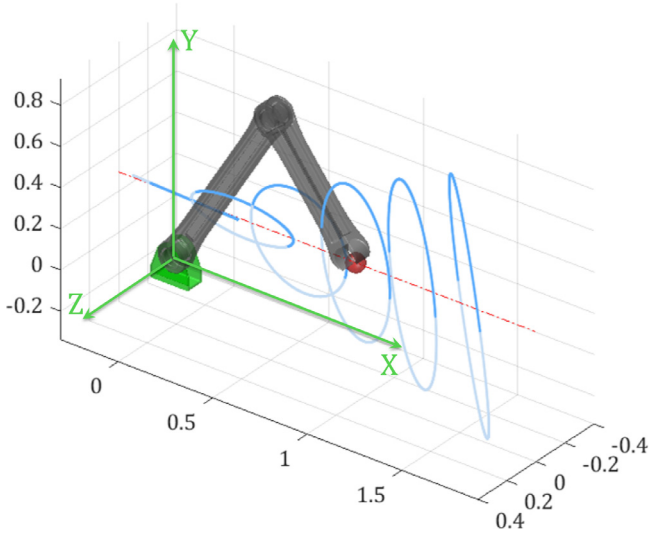

Fig. 2. Kinetic energy ellipses of the two-link manipulator along *X*-axis.

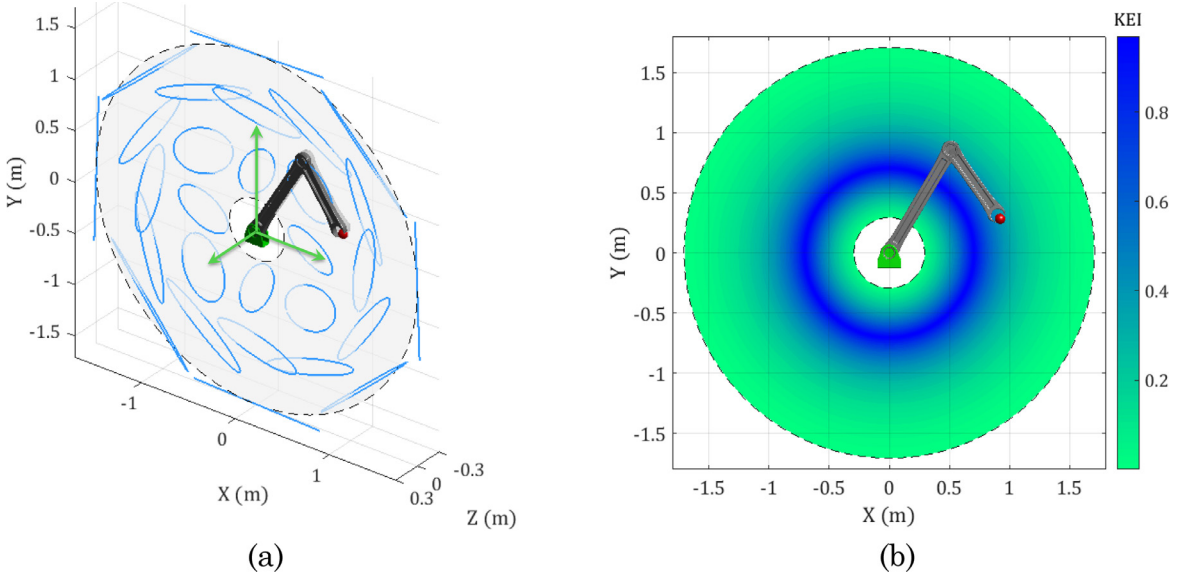

Fig. 3. a) Kinetic energy ellipses over the workspace, b) Contours of KEI.

The relation ${}^{\mathcal{P}}\mathbf{k}_P = {}^{\mathcal{P}}\mathbf{E}\dot{\mathbf{q}}$ maps the hyper-sphere of $\dot{\mathbf{q}} \cdot \dot{\mathbf{q}} = 1$ in joint space to a hyper-ellipsoid. The direction of the principle diameters are obtained as:

$$ {}^{\mathcal{P}}\mathbf{k}_P^* = \frac{1}{\sqrt{2}} \begin{bmatrix} M_P^{0.5\,\mathcal{P}}\mathbf{J}_P \\ {}^{\mathcal{P}}\mathbf{I}_P^{0.5\,\mathcal{P}}\mathbf{J}_P \end{bmatrix} \dot{\mathbf{q}}^* \tag{20} $$

Note that, the direction of ${}^{\mathcal{P}}\mathbf{k}_P^*$ does not provide any physical quantity. However, its magnitude resembles the square root of the kinetic energy of the payload, $|{}^{\mathcal{P}}\mathbf{k}_P^*| = \sqrt{\mathcal{K}_P} = \sqrt{\Lambda^*}$ where, $|.|$ stands for Euclidean norm of the vector. It is desired to uniformize the kinetic energy transferred to the payload for all the feasible joint velocities. If the hyper-ellipsoid of the kinetic energy becomes a hyper-sphere, an identical kinetic energy is transferred to the payload for all the feasible joint velocities. On the other hand, when the hyper-ellipsoid loses one of its dimensions and reduces to a hyper-surface, no kinetic energy is transferred to the payload for some specific values of joint velocities. Therefore, it is not sufficient to merely consider the maximum value of $\mathcal{K}_P$. To resolve this issue the local kinetic energy index, KEI $\in [0, 1]$, is defined as,

$$ \mathrm{KEI} = \frac{1}{\sqrt{\Lambda^*_{max}/\Lambda^*_{min}}} \tag{21} $$

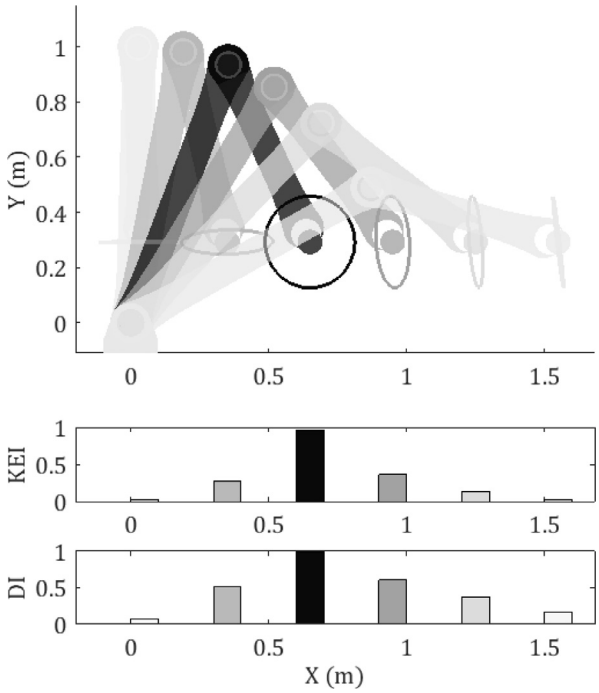

Fig. 4. KEI and DI indices for a two-link manipulator along a straight path.

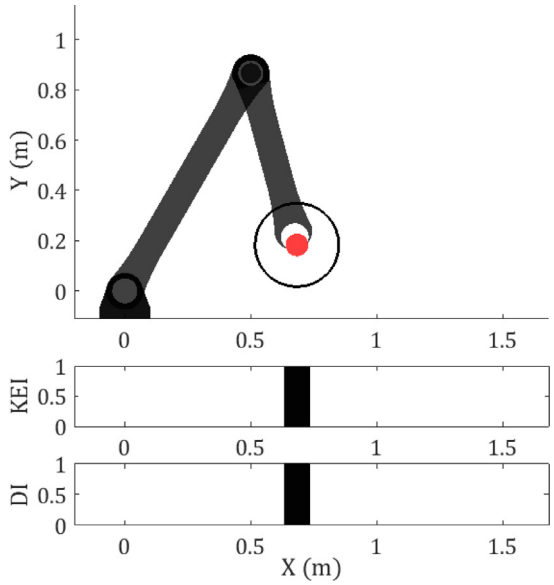

Fig. 5. Isotropic configuration of the two-link robot with respect to DI and KEI indices.

Regarding the kinetic energy transfer, a small value of KEI indicates that the robot is in an undesirable configuration. Therefore, for a given payload, it is desired to design the robots such that the KEI is close to unity over the entire workspace.

4. Case studies

4.1. Two-Link serial manipulator

Fig. 1 shows a serial planar manipulator in which a spherical payload is attached to the EE. The manipulator is comprised of two links with lengths of L_1 and L_2 located at the angles of q_1 and q_2, respectively. Clearly, the robot has two degrees of

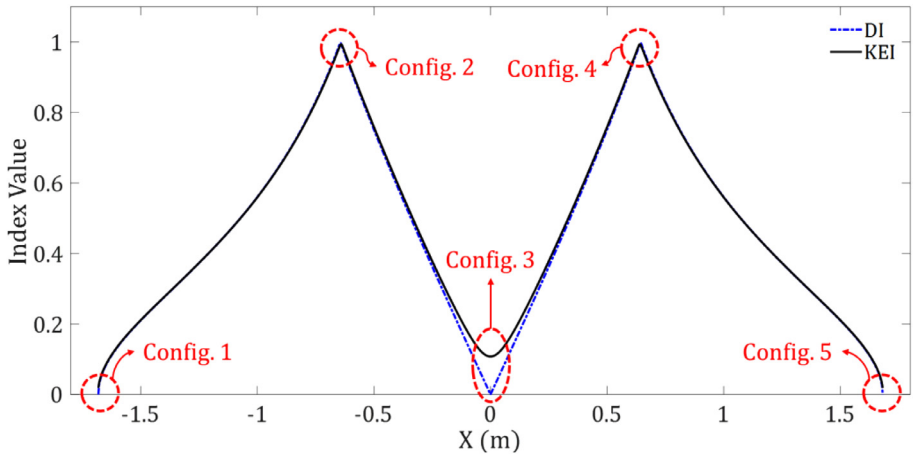

Fig. 6. DI and KEI curves for the two-link serial manipulator.

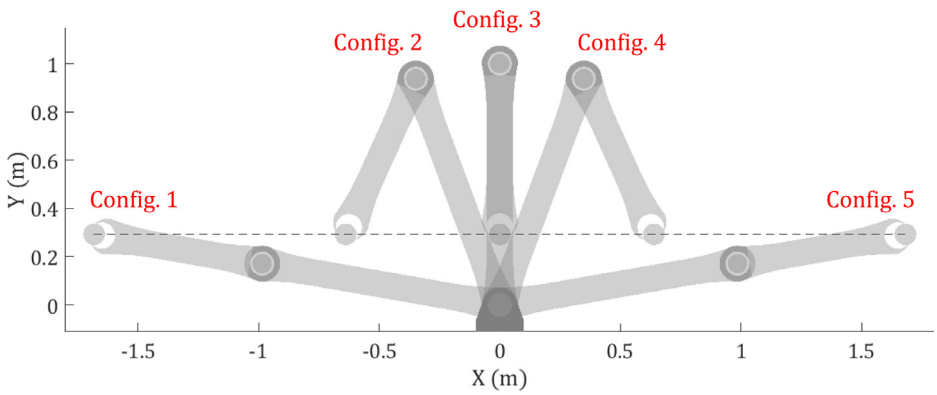

Fig. 7. Two link serial manipulator at singular and isotropic configurations.

freedom, x and y. However an extra generalized coordinate, ϕ, is considered in order to define the vector of oriented kinetic energy.

The Jacobian matrix, ${}^{\mathcal{B}}\mathbf{J}_P$, maps the vector of joints velocities, $\dot{\mathbf{q}} = [\ \dot{q}_1 \quad \dot{q}_2\ ]^T$, to the vector of the generalized velocity of the payload, ${}^{\mathcal{B}}\dot{\mathbf{X}} = [\ \dot{x} \quad \dot{y}\ ]^T$ as,

$$ {}^{\mathcal{B}}\dot{\mathbf{X}} = {}^{\mathcal{B}}\mathbf{J}_P\dot{\mathbf{q}} \tag{22} $$

where, the superscript $\{B\}$ indicates the base coordinate system and the Jacobian matrix is calculated as,

$$ {}^{\mathcal{B}}\mathbf{J}_P = \begin{bmatrix} -L_1\sin q_1 - L_2\sin(q_1+q_2) & -L_2\sin(q_1+q_2) \\ L_1\cos q_1 + L_2\cos(q_1+q_2) & L_2\cos(q_1+q_2) \end{bmatrix}_{2\times 2} \tag{23} $$

${}^{\mathcal{B}}\dot{\mathbf{X}}$ defines the translational DOFs of the manipulator. Therefore, ${}^{\mathcal{B}}_{T}\mathbf{J}_P = {}^{\mathcal{B}}\mathbf{J}_P$. However, the calculation of the kinetic energy requires the orientation of the payload, ϕ, which is simply equal to summation of the joint angles, $\phi = q_1 + q_2$. Therefore, ${}^{\mathcal{B}}_{R}\mathbf{J}_P = [\ 1 \quad 1\ ]$.

In this case, the moment of inertia of the spherical payload is invariant with respect to the orientation of the coordinate system. Hence, the coordinate system $\{\mathcal{P}\}$ is located at the payload position and aligned with the base coordinate system. Therefore, all the vectors and matrices can be expressed in $\{\mathcal{B}\}$. Finally, the linear and rotational velocities of the payload are obtained as,

$$ {}^{\mathcal{B}}\mathbf{V}_P = {}^{\mathcal{B}}_{T}\mathbf{J}_P\dot{\mathbf{q}} \tag{24} $$

$$ {}^{\mathcal{B}}\boldsymbol{\Omega}_P = {}^{\mathcal{B}}_{R}\mathbf{J}_P\dot{\mathbf{q}} \tag{25} $$

4.1.1. Kinetic energy ellipsoid

Considering the constraint of $\dot{\mathbf{q}} \cdot \dot{\mathbf{q}} = 1$, the maximum and minimum kinetic energies transferred to the payload are calculated in this section. The kinematic and dynamic parameters of the two-link serial manipulator are chosen as $L_1 = 1.00\ m$, $L_2 = 0.71\ m$ and $M_P = 10\ kg$.

The payload can only take rotations about the Z-axis, so just the third component of the inertia tensor, ${}^{\mathcal{B}}I_{P,33}$, appears in motion equations of the robot. The inertia of the payload is a function of its shape and mass. In this case, the payload is a solid sphere and its inertia is calculated as, ${}^{\mathcal{B}}I_{P,33} = \frac{2}{5}M_P r_P^2$. The 3D ellipses of the kinetic energy for the two-link robot are illustrated in Fig. 2. In this case, the payload is moved on a straight line along X-axis while the Y coordinate is held constant at $Y = L_1 - L_2$. The directions of the major and minor axes of the ellipses are calculated according to Eq. (20).

As shown in Fig. 2, when the robot is fully stretched or fully retracted, the kinetic energy ellipses approach to lines. This indicates that in these configurations some combinations of joint velocities could be found which do not transfer any kinetic energy to the payload. However, when the kinetic energy ellipses approach to circles, the same kinetic energy is transferred to the payload for all the feasible joint velocities. Note that, despite the planar motion of the robot, the ellipses do not lay in XY plane. The darker parts of the ellipses in Fig. 2, have positive Z values while the lighter parts have negative Z values.

Fig. 3a depicts the kinetic energy ellipses over the entire workspace of the robot. At the workspace boundary the ellipses approached to lines indicating bad configurations considering the transfer of kinetic energy. The contours of the kinetic energy index are shown in Fig. 3b for the entire workspace of the robot. The circular contours in Fig. 3b indicate that KEI is invariant with respect to the rotations of the first axis of the robot.

The dexterity index, DI, is one of the most important performance indices used for evaluating the maneuverability of the manipulators in different directions [26,27]. For a given manipulator, DI is defined as,

$$\mathrm{DI} = \frac{1}{\sqrt{\lambda^*_{max}/\lambda^*_{min}}} \tag{26}$$

where, $\lambda^*_{\max}$ and $\lambda^*_{\min}$ are the maximum and minimum eigenvalues of the matrix $\mathbf{G} = {}^{\mathcal{B}}\mathbf{J}_P^{T\,\mathcal{B}}\mathbf{J}_P$. When the DI value is close to 0, the EE will not be able to maneuver along some directions. On the other hand, a DI value of unity indicates a dexterous manipulator.

Fig. 4 compares KEI and DI for the two-link serial manipulator along a straight path parallel to the x axis. The ellipses shown in Fig. 4 are the translational manipulability ellipses. As mentioned before, the KEI ellipses for the two link serial manipulator do not fall within the plane of motion. Considering this fact and to avoid a messy figure, KEI values are presented through the colors in Fig. 4. A darker robot indicates a better configuration with respect to the kinetic energy index.

4.1.2. Isotropic configuration

The concept of isotropy was initially proposed by Salisbury and Craig for the optimal design of the fingers of a mechanical arm [8]. The isotropy concept is based on the condition number of the Jacobian matrix. In an isotropic configuration, the condition number of the Jacobian matrix is equal to unity or, equivalently, all the eigenvalues of the matrix $\mathbf{G} = {}^{\mathcal{B}}\mathbf{J}_P^{T\,\mathcal{B}}\mathbf{J}_P$ are identical [28–30]. In other words, in an isotropic configuration, the manipulability ellipse becomes a circle. The isotropic configuration of the two-link serial robot can be found by equating $\mathbf{G} = {}^{\mathcal{B}}\mathbf{J}_P^{T\,\mathcal{B}}\mathbf{J}_P$ to $\sigma_G^2\mathbf{I}$as,

$$\mathbf{G} = {}^{\mathcal{B}}\mathbf{J}_P^{T\,\mathcal{B}}\mathbf{J}_P = \sigma_G^2\mathbf{I} \tag{27}$$

where, σ_G is a constant and $\mathbf{I}_{2\times 2}$ is the unity matrix. Substituting Eq. (23) in Eq. (27) yields,

$$\mathbf{G} = \begin{bmatrix} L_1^2 + 2L_1L_2\cos q_2 + L_2^2 & L_2^2 + L_1L_2\cos q_2 \\ L_2^2 + L_1L_2\cos q_2 & L_2^2 \end{bmatrix} = \begin{bmatrix} \sigma_G^2 & 0 \\ 0 & \sigma_G^2 \end{bmatrix} \tag{28}$$

Therefore, the isotropic configuration of the two link serial manipulator with respect to DI, is obtained as,

$$L_1 = \sqrt{2}L_2, \quad q_2 = \cos^{-1}\left(-\frac{\sqrt{2}}{2}\right) \tag{29}$$

Considering the kinetic energy index, KEI, the isotropic configuration of the two-link serial manipulator can be found by following a similar procedure and solving Eq. (30),

$$\mathcal{K} = {}^{\mathcal{P}}\mathbf{E}^{T\,\mathcal{P}}\mathbf{E} = \sigma_K^2\mathbf{I} \tag{30}$$

σ_K in Eq. (30) is a constant and $\mathbf{I}_{2\times 2}$ is again the unity matrix. Substituting Eq. (12) in Eq. (30) yields,

$$\begin{aligned} \mathcal{K} &= \frac{1}{2}\begin{bmatrix} {}^{\mathcal{B}}I_{P,33} + M_P\left(L_1^2 + L_2^2 + 2L_1L_2\cos q_2\right) & {}^{\mathcal{B}}I_{P,33} + M_P\left(L_2^2 + L_1L_2\cos q_2\right) \\ {}^{\mathcal{B}}I_{P,33} + M_P\left(L_2^2 + L_1L_2\cos q_2\right) & {}^{\mathcal{B}}I_{P,33} + M_PL_2^2 \end{bmatrix} \\ &= \begin{bmatrix} \sigma_K^2 & 0 \\ 0 & \sigma_K^2 \end{bmatrix} \end{aligned} \tag{31}$$

Finally, the isotropic configurations of the two-link serial manipulator with respect to KEI, are obtained as,

$$L_1 \le 2L_2,\ q_2 = \cos^{-1}\left(-\frac{L_1}{2L_2}\right) \tag{32}$$

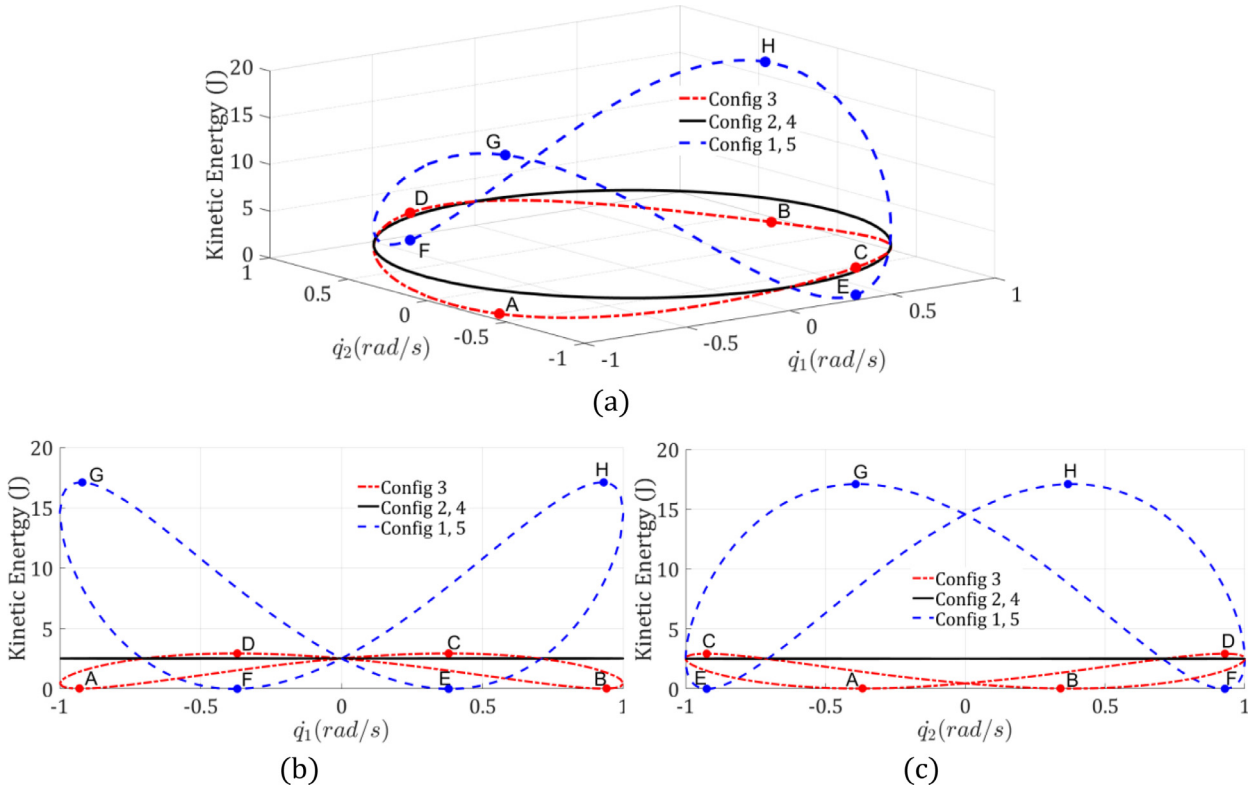

Fig. 8. Kinetic energy variations for the five specified configurations.
a) 3D view, b) KEI versus $\dot{q}_1$, c) KEI versus $\dot{q}_2$.

Comparing Eq. (29) with Eq. (32) reveals that if a configuration of the robot meets the DI isotropy conditions, it will also meet the KEI isotropy conditions. However, the reverse is not true. In other words, some configurations may be found which meet the KEI isotropy conditions while violating the DI isotropy condition. Fig. 5 shows a configuration of the two-link robot which is simultaneously isotropic with respect to DI and KEI.

Fig. 6 shows DI and KEI curves for the two link serial manipulator. The X coordinate of the EE is changed between two fully stretched configurations while its Y coordinate is kept constant. Five configurations of the manipulator are specified in Fig. 6, named as Config. 1∼5. Config. 1 and Config. 5 correspond to singular configurations where the robot is fully stretched. Config. 3 represents the fully retracted singular configuration. Config. 2 and Config. 4 correspond to isotropic configurations of the manipulator. Fig. 7 depicts the robot in the specified configurations.

According to Fig. 7, the kinetic energy index has a small value in Config. 1, 3 & 5. This indicates that some feasible joint velocities can be found where a very small kinetic energy is transferred to the payload. In Config. 2 & 4 the KEI is equal to unity, indicating that for all feasible joint velocities a uniform kinetic energy is transferred to the payload.

The variation of the transferred kinetic energy for the five specified configurations is shown in Fig. 8. The uniformity of the transferred kinetic energy in the isotropic configurations (Config. 2 & 4) is evident from Fig. 8 where the corresponding curve forms a flat circle. However, the corresponding curves of singular configurations shows multiple ups and downs, indicating the fluctuations in the kinetic energy. As marked in Fig. 8, the points A, B, E and F denote the combinations of the joint velocities which lead to the minimum transferred kinetic energy, whereas the points C, D, G and H denote the maximum transferred kinetic energy.

4.2. Parallel 3-RRR manipulator

Fig. 9 depicts a schematic view of a 3-RRR planar parallel manipulator. The 3-RRR parallel robot is composed of three identical kinematic chains each containing three successive rotational joints (RRR). The moving platform of the robot is connected to the base through two successive links with lengths of l_i and L_i. As shown in Fig. 9, the payload is located at the center of the triangular moving platform.

The pose of the payload can be fully determined by defining the vector of the generalized coordinates as ${}^{\mathcal{B}}\mathrm{X} = [\ x \quad y \quad \phi\ ]^T$. The parameters x and y define the location of the payload and the parameter ϕ defines its orientation.

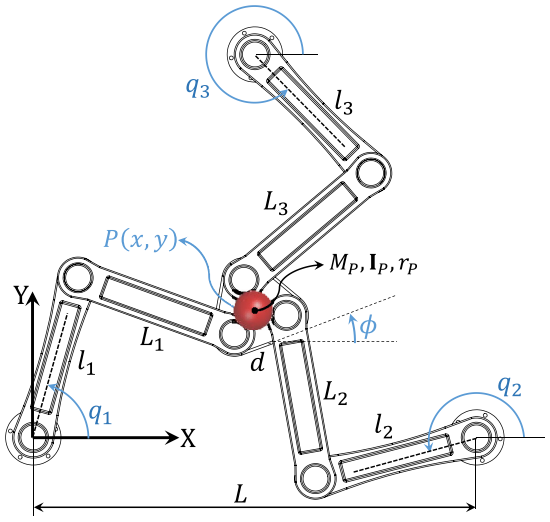

Fig. 9. 3-RRR planar manipulator.

Table 1
Kinematic and dynamic parameters of the 3-RRR parallel manipulator.

Parameters	Value	Parameter	Value
L	0.8 m	d	0.1 m
l_i	0.3 m	M_P	10 kg
L_i	0.3 m	${}^{\mathcal{P}}I_{P,33}$	0.0042 $kg.m^2$

The vector of the generalized velocity of the payload is defined in the coordinate system $\{\mathcal{B}\}$ as ${}^{\mathcal{B}}\dot{\mathrm{X}} = [\ \dot{x} \quad \dot{y} \quad \dot{\phi}\ ]^{\mathrm{T}}$. The Jacobian matrix ${}^{\mathcal{B}}\mathrm{J}_P$ maps the joint velocity vector, $\dot{\mathrm{q}} = [\dot{q}_1 \quad \dot{q}_2 \quad \dot{q}_3]^{\mathrm{T}}$, to ${}^{\mathcal{B}}\dot{\mathrm{X}}$ as,

$$ {}^{\mathcal{B}}\dot{\mathrm{X}} = {}^{\mathcal{B}}\mathbf{J}_P\dot{\mathbf{q}} \tag{33} $$

The coordinate system $\{\mathcal{P}\}$ is located at the center of the payload with axes aligned with the principle axes of the payload. Using the rotation matrix from $\{\mathcal{B}\}$ to $\{\mathcal{P}\}$, ${}^{\mathcal{P}}_{\mathcal{B}}\mathcal{R}$, the generalized velocity vector of the payload can be calculated in the coordinate system $\{\mathcal{P}\}$ as,

$$ {}^{\mathcal{P}}\dot{\mathrm{X}} = {}^{\mathcal{P}}_{\mathcal{B}}\mathcal{R}\,{}^{\mathcal{B}}\dot{\mathrm{X}} = {}^{\mathcal{P}}_{\mathcal{B}}\mathcal{R}\,{}^{\mathcal{B}}\mathbf{J}_P\dot{\mathbf{q}} = {}^{\mathcal{P}}\mathbf{J}_P\dot{\mathbf{q}} \tag{34} $$

Decomposing the Jacobian matrix into translational and rotational parts, the linear and angular velocity of the payload can be calculated as,

$$ {}^{\mathcal{P}}\mathbf{V}_P = {}^{\mathcal{P}}_{T}\mathbf{J}_P\dot{\mathbf{q}} \tag{35} $$

$$ {}^{\mathcal{P}}\boldsymbol{\Omega}_P = {}^{\mathcal{P}}_{R}\mathbf{J}_P\dot{\mathbf{q}} \tag{36} $$

The translational and rotational Jacobian matrices of the 3-RRR robot, ${}^{\mathcal{P}}_{T}\mathbf{J}_P$ and ${}^{\mathcal{P}}_{R}\mathbf{J}_P$, are obtained as,

$$ {}^{\mathcal{P}}_{T}\mathbf{J}_P = \frac{1}{(\mathbf{a}_1\times\mathbf{a}_2)\cdot\mathbf{a}_3}\,{}^{\mathcal{P}}_{B}\mathcal{R}\begin{bmatrix}(\mathbf{a}_2\times\mathbf{a}_3)\cdot\mathbf{b}_1 & (\mathbf{a}_2\times\mathbf{a}_3)\cdot\mathbf{b}_2 & (\mathbf{a}_2\times\mathbf{a}_3)\cdot\mathbf{b}_2\\ (\mathbf{a}_3\times\mathbf{a}_1)\cdot\mathbf{b}_1 & (\mathbf{a}_3\times\mathbf{a}_1)\cdot\mathbf{b}_2 & (\mathbf{a}_3\times\mathbf{a}_1)\cdot\mathbf{b}_3\end{bmatrix}b_3 \tag{37} $$

$$ {}^{\mathcal{P}}_{R}\mathbf{J}_P = \frac{1}{(\mathbf{a}_1\times\mathbf{a}_2)\cdot\mathbf{a}_3}\,{}^{\mathcal{P}}_{B}\mathcal{R}\Big[(\mathbf{a}_1\times\mathbf{a}_2)\cdot\mathbf{b}_1 \quad (\mathbf{a}_1\times\mathbf{a}_2)\cdot\mathbf{b}_2 \quad (\mathbf{a}_1\times\mathbf{a}_2)\cdot\mathbf{b}_3\Big] \tag{38} $$

The vectors $\mathbf{a}_i$ and $\mathbf{b}_i$ are given in Appendix A.

Having obtained the translational and rotational Jacobian matrices, Eq. (13) can be used to calculate the kinetic energy matrix. $\mathcal{K}$ is a 3 by 3 matrix and has three eigenvalues of $\Lambda^*_{\min}$, Λ^*_{mid} and $\Lambda^*_{\max}$ and three corresponding eigenvectors of $\dot{\mathbf{q}}^*_{\min}$, $\dot{\mathbf{q}}^*_{\mathrm{mid}}$ and $\dot{\mathbf{q}}^*_{\max}$. Using the parameter values given in Table 1, Fig. 10 shows the kinetic energy ellipsoids of the 3-RRR robot over its entire workspace for $\phi = 0$.

The contours of KEI index for the 3-RRR parallel robot are depicted in Fig. 11. The payload rotation is changed from $\phi = -30^o$ to $\phi = +30^o$. The results clearly show that KEI value is minimum at workspace boundaries and increases at the center of the workspace.

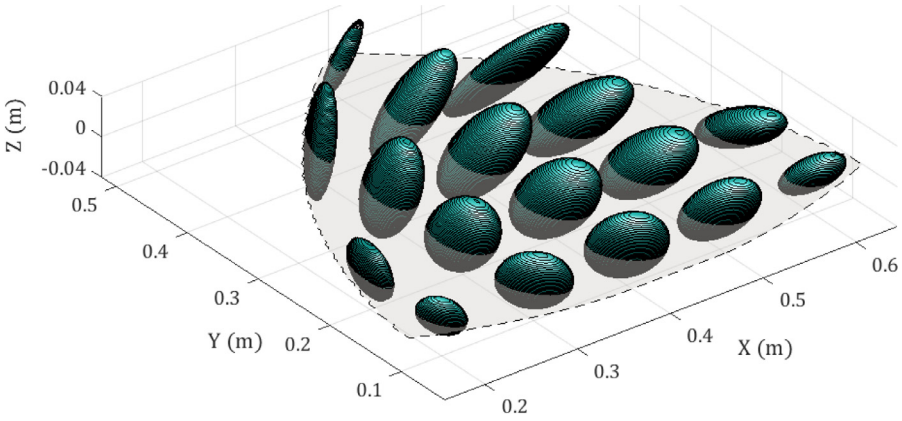

Fig. 10. Kinetic energy ellipsoids of the 3-RRR robot over the workspace for $\phi = 0$.

In the following, the performance of the kinetic energy index is further evaluated through comparison with the dexterity index. Since the robot has mixed translational and rotational DOFs, its Jacobian matrix is non-homogeneous. To resolve the non-homogeneity issue, some references propose to divide the elements of the Jacobian matrix with a unit length by a characteristic length. Different methods are proposed for choosing the characteristic length. Some references propose to choose the characteristic length in a way that the isotropy conditions are satisfied for the robot [31]. However, solving the isotropy conditions is not always possible especially for parallel manipulators. Therefore, it is generally suggested to use a constant length as the characteristic length. This constant length should be a parameter of the robot geometry which represents the overall size of the robot.

Fig. 12 compares the KEI and DI values for the 3-RRR parallel robot. The moving platform is located concentric with the base platform while its orientation is changed from $\phi = -90^o$ to $\phi = 90^o$. DI curves are shown for four cases. In the first case, the non-homogenized Jacobian matrix is used. In the second case, the Jacobian matrix is homogenized using a constant length which is chosen as the size of the moving platform side, d. In the third case, the characteristic length is obtained by solving isotropy conditions. Hereafter this length is denoted as L_{iso}. According to [31] the isotropy configuration for the 3-RRR robot is obtained when, (1) the base and moving platforms are concentric equilateral triangles, (2) corresponding legs have the same lengths, (3) the angles between the legs are equal. Meeting the above conditions, the characteristic length, L_{iso}, could be found as a function of EE orientation. In the fourth case, ideal isotropic length, L_{ideal} is considered for homogenizing the Jacobian matrix. This characteristic length is a constant value which is obtained when the manipulator is as far away as possible from a parallel singularity [32].

As shown in Fig. 12, the DI curve for the non-homogenized Jacobian matrix shows that for $\phi = -40.5^o$, the robot is in a singular configuration. Due to the non-homogeneity of the Jacobian matrix, the DI values will change by altering the length unit. Homogenizing the Jacobian matrix with a constant length, e.g. d, the DI curve follows the same trend as the non-homogenized DI curve and detects the singularity neighborhood. As intuitively expected, the arbitrariness of choosing a constant length as the characteristic length leads to different values for DI index. Using L_{iso} to homogenize the Jacobian matrix, the isotropy conditions are successfully satisfied and a unit condition number is obtained for different EE orientations. However, this method fails in detecting the singularity neighborhood. Perhaps the best way to normalize the Jacobian matrix is to use L_{ideal}, but obtaining this value is very complicated, especially for parallel robots.

The dynamic dexterity index, DDI, is another useful performance index which evaluates the dynamic dexterity of robots [33,34]. A DDI value close to unity indicates that, for feasible joint torques, the robot can be easily accelerated in all directions. This index is calculated as,

$$\mathrm{DDI} = \frac{\sigma_{min}\left({}^{\mathcal{B}}\mathbf{J}_P\mathbf{M}^{-1}\right)}{\sigma_{max}\left({}^{\mathcal{B}}\mathbf{J}_P\mathbf{M}^{-1}\right)} \tag{39}$$

where, $\mathbf{M}$ is the inertia matrix of the robot. Neglecting the inertia of the connecting links, the inertia matrix of the robot is equal to the matrix $\mathcal{K}$ in Eq. (13). σ_{max} and σ_{min} represents the maximum and minimum singular values of the ${}^{\mathcal{B}}\mathbf{J}_P\mathbf{M}^{-1}$ respectively.

Fig. 12 indicates that the kinetic energy index changes with the payload orientation and successfully detects the singularity neighborhood of the robot. This index considers both translational and rotational motions of payload and does not suffer from non-homogeneity issues. Fig. 13, shows the configuration of the robot corresponding to the minimum value of KEI which is also a singular configuration of the robot. In this configuration, which is referred to as parallel singularity, the three lines along the second links intersect in a common point [32].

The two configurations of the 3-RRR robot corresponding to the maximum KEI values are depicted in Fig. 14.

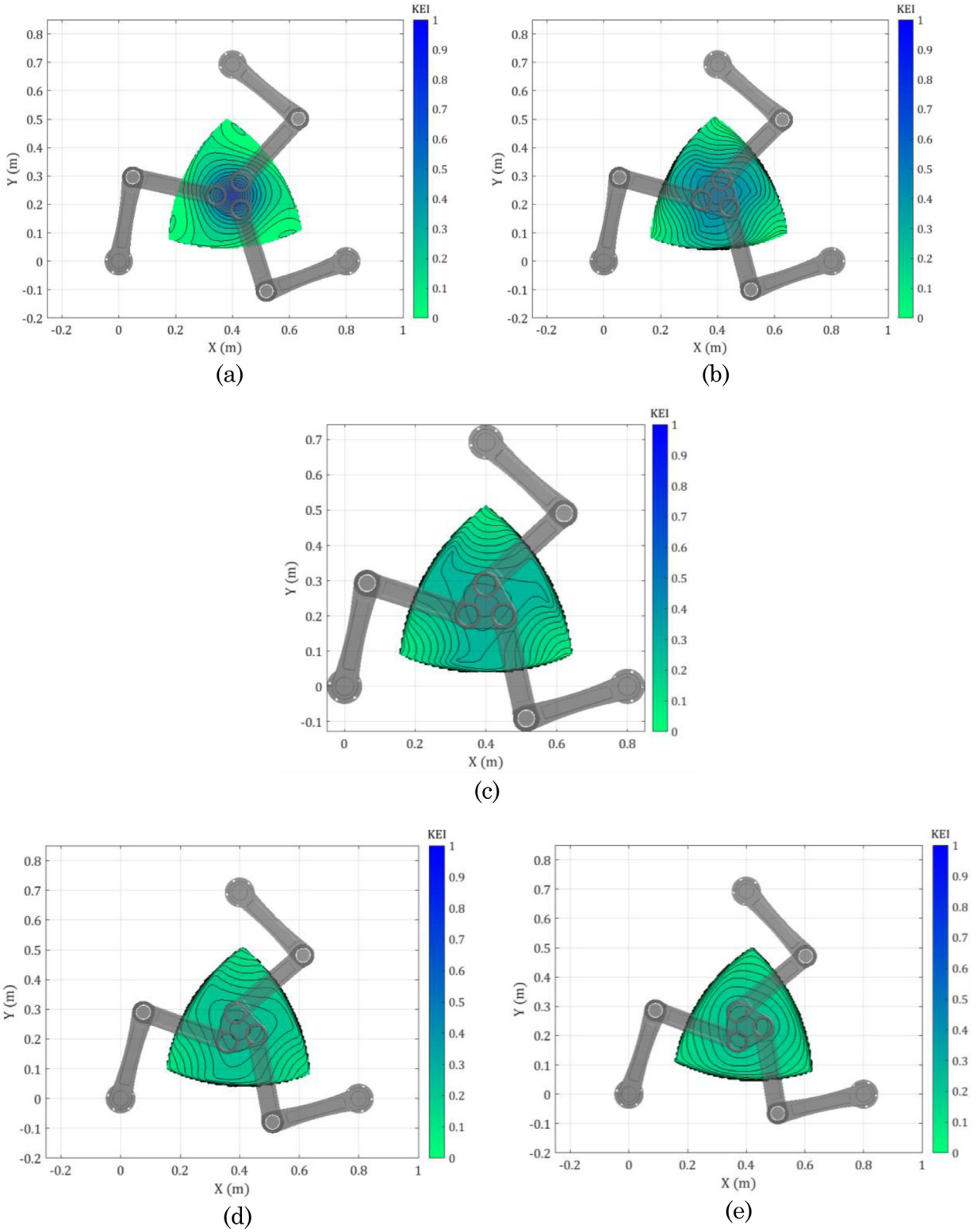

Fig. 11. KEI contours for the 3-RRR parallel manipulator
a) $\phi = -30^o$, b) $\phi = -15^o$, c) $\phi = 0^o$, d) $\phi = 15^o$, e) $\phi = 30^o$.

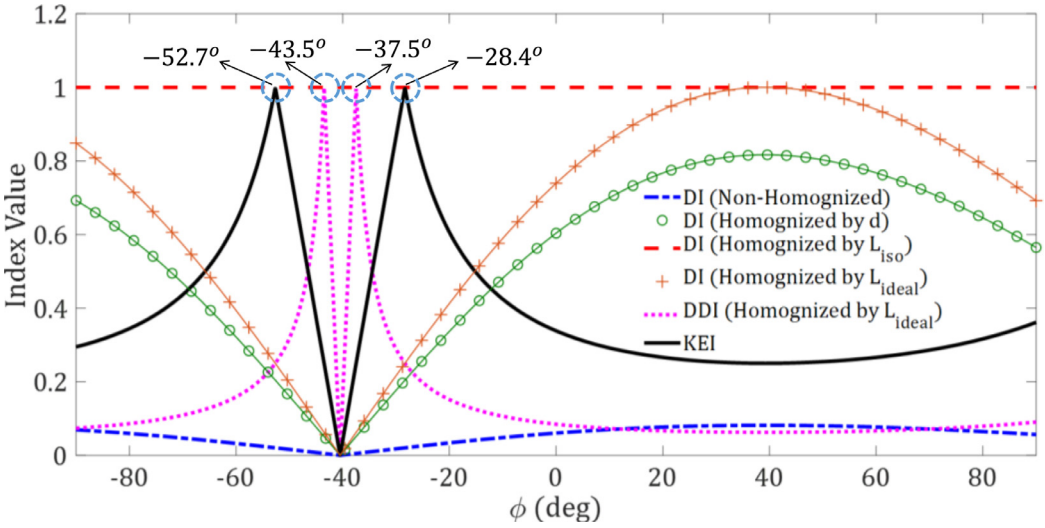

Fig. 12. Comparing KEI, DI and DDI indices for the 3-RRR manipulator.

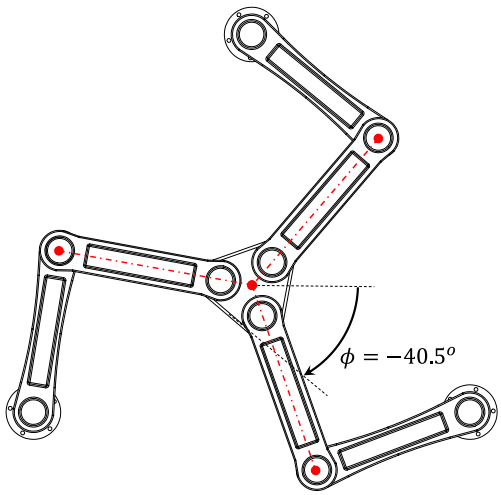

Fig. 13. Minimum KEI configuration for 3-RRR robot.

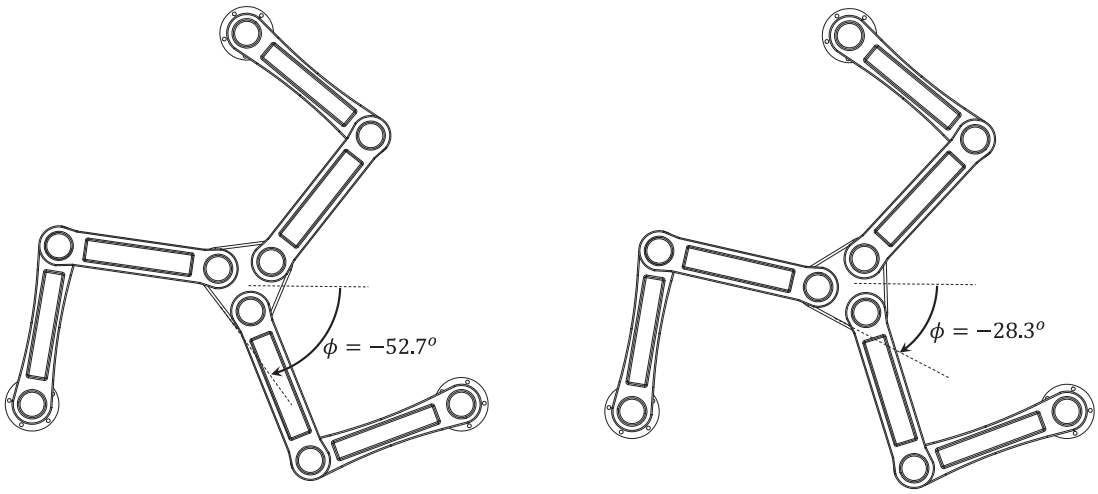

Fig. 14. Maximum KEI configurations for 3-RRR robot.

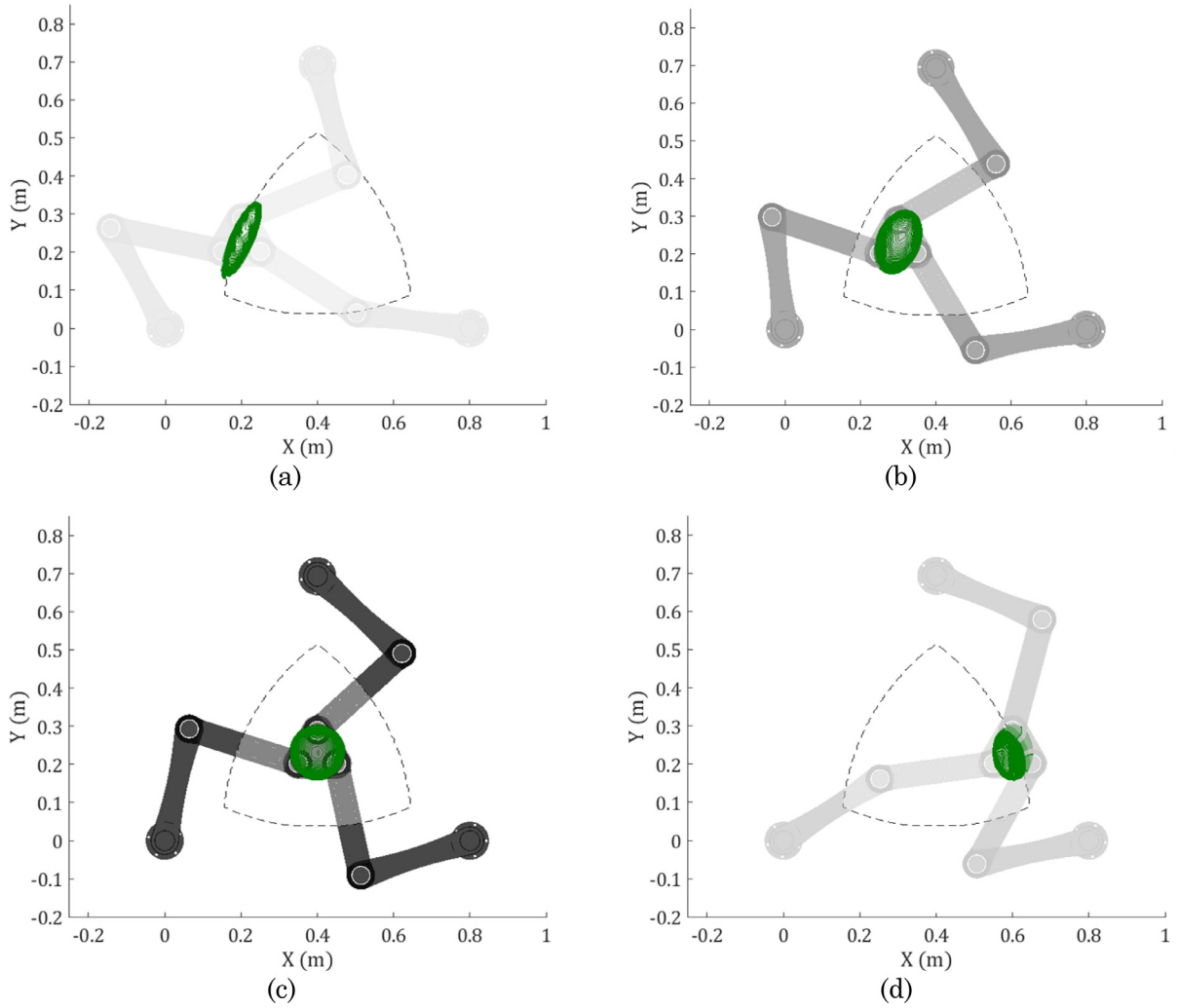

Fig. 15. DI and KEI indices for the 3-RRR parallel manipulator a) DI = 0.25, KEI = 0.22, b) DI = 0.55, KEI = 0.27, c) DI = 0.74, KEI = 0.34, d) DI = 0.23, KEI = 0.23.

Fig. 15 compares the KEI and DI indices for the 3-RRR parallel manipulator. The Jacobian matrix is homogenized by L_{ideal} for calculating the dexterity index. The EE is moved along the x-axis while its Y coordinate is fixed at $Y = 0.23\ m$ and the EE rotation is zero. The ellipsoids in Fig. 15 indicate the DI index. As the ellipses get closer to the circle, the robot in a better configuration with respect to DI index. KEI index is shown through colors. A darker color shows a higher KEI value.

5. Conclusion

In this paper, the concepts of rms velocity norm and generalized inertia ellipsoid are used to propose a payload specific index is presented for performance evaluation of manipulators. For the rms velocity norm the weighting function is chosen as the mass density of the payload, While for GIE only the dynamic properties of the payload are considered. These special cases, where rms velocity norm and GIE simplify to the kinetic energy of the payload, are used to define a payload specific kinetic energy index, KEI. This index measures the uniformity of kinetic energy transferred to the payload. Unlike the traditional performance indices, KEI considers both of the translational and rotational motions of the manipulator simultaneously. Moreover, this index is dimensionally homogeneous and is independent from the units used for longitudinal and angular variables. KEI is also independent from scaling the robot dimensions. A unit value of KEI indicates that, for all the feasible joint velocities, a uniform kinetic energy is transferred to the payload. On the other hand, in the case of a small KEI value, the transferred kinetic energy drastically varies for different combinations of the feasible joint velocities. Performance of the proposed index is evaluated for two cases of a two-link serial manipulator and a 3-RRR parallel robot. The kinetic energy ellipsoids and the contours of the KEI values are depicted over the entire workspace of the two robots. It is seen that the ellipsoids are stretched at the workspace boundaries designating that the kinetic energy is not transferred to the

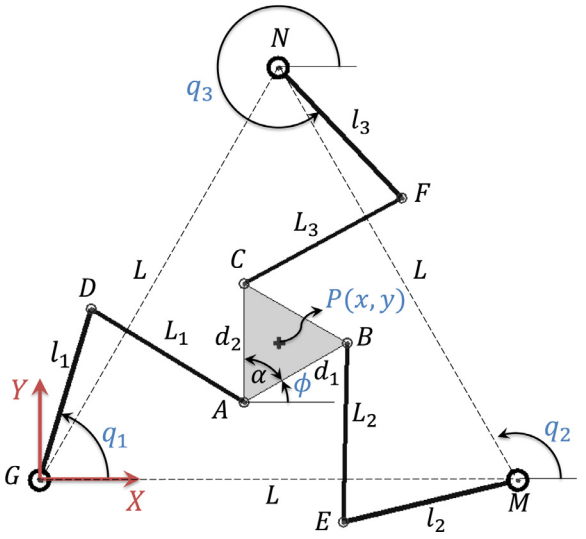

Fig. A.1. Schematic of the 3-RRR parallel manipulator.

payload for some feasible joint velocities. The provided results indicate that the proposed index can be confidently used in optimizing the robot structure for a given payload with specified dynamic properties.

Declarations of interest

None.

Appendix A.

Fig. A.1 depicts a schematic view of a 3-RRR parallel robot and defines its kinematic parameters.
Considering the velocity equations for the payload, the Jacobian matrix of the robot can be expressed as,

$$\mathrm{A}\dot{\mathrm{X}} = \mathrm{B}\dot{\mathrm{q}} \Rightarrow \dot{\mathrm{X}} = \mathrm{J}\dot{\mathrm{q}};\ \mathrm{J} = \mathrm{A}^{-1}\mathrm{B} \tag{A.1}$$

where,

$$\mathbf{A} \equiv \begin{bmatrix}\mathbf{a}_1 & \mathbf{a}_2 & \mathbf{a}_3\end{bmatrix},\quad \dot{\mathbf{X}} = \begin{bmatrix}\dot{x} & \dot{y} & \dot{\phi}\end{bmatrix}^T \tag{A.2}$$

$$\mathbf{Q} \equiv \begin{bmatrix}\mathbf{b}_1 & \mathbf{b}_2 & \mathbf{b}_3\end{bmatrix},\quad \dot{\mathbf{q}} = \begin{bmatrix}\dot{q}_1 & \dot{q}_2 & \dot{q}_3\end{bmatrix}^T \tag{A.3}$$

in which [22],

$$\mathbf{a}_1 = \begin{bmatrix} x_A - l_1\cos q_1 \\ x_A + d_1\cos\phi - x_M - l_2\cos q_2 \\ x_A + d_2\cos(\phi+\alpha) - x_N - l_3\cos q_3 \end{bmatrix} \tag{A.4}$$

$$\mathbf{a}_2 = \begin{bmatrix} y_A - l_1\sin q_1 \\ y_A + d_1\sin\phi - l_2\sin q_2 \\ y_A + d_2\sin(\phi+\alpha) - y_N - l_3\sin q_3 \end{bmatrix} \tag{A.5}$$

$$\mathbf{a}_3 = \begin{bmatrix} (\mathbf{k}\times\mathbf{r}_{A/P})\cdot\mathbf{r}_{A/D} \\ (\mathbf{k}\times\mathbf{r}_{B/P})\cdot\mathbf{r}_{B/E} \\ (\mathbf{k}\times\mathbf{r}_{C/P})\cdot\mathbf{r}_{C/F} \end{bmatrix} \tag{A.6}$$

$$\mathbf{b}_1 = \begin{bmatrix} (\mathbf{k}\times\mathbf{r}_{D/G})\cdot\mathbf{r}_{A/D} \\ 0 \\ 0 \end{bmatrix},\quad \mathbf{b}_2 = \begin{bmatrix} 0 \\ (\mathbf{k}\times\mathbf{r}_{E/M})\cdot\mathbf{r}_{B/E} \\ 0 \end{bmatrix},\quad \mathbf{b}_3 = \begin{bmatrix} 0 \\ 0 \\ (\mathbf{k}\times\mathbf{r}_{F/N})\cdot\mathbf{r}_{C/F} \end{bmatrix} \tag{A.7}$$

References

[1] H. Asada, Dynamic analysis and design of robot manipulators using inertia ellipsoids, in: Robotics and Automation. Proceedings. 1984 IEEE International Conference on, 1984, pp. 94–102.
[2] Q. Lin, J.W. Burdick, E. Rimon, Constructing minimum deflection fixture arrangements using frame invariant norms, IEEE Trans. Autom. Sci. Eng. 3 (2006) 272–286.
[3] S. Patel, T. Sobh, Manipulator performance measures-a comprehensive literature survey, J. of Intell. Rob. Sys. 77 (2015) 547–570.
[4] S. Hwang, H. Kim, Y. Choi, K. Shin, C. Han, Design optimization method for 7 DOF robot manipulator using performance indices, Int. J. Precis. Eng. Manuf. 18 (2017) 293–299.
[5] J. Enferadi, R. Nikrooz, The performance indices optimization of a symmetrical fully spherical parallel mechanism for dimensional synthesis, J. Intell. Rob. Sys. (2017) 1–17.
[6] J.F. O'Brien, F. Jafari, J.T. Wen, Determination of unstable singularities in parallel robots with N arms, IEEE Trans. Rob. 22 (2006) 160–167.
[7] T. Yoshikawa, Analysis and control of robot manipulators with redundancy, Rob. Res. First Int. Symp., MIT press (1984) 735–747.
[8] J.K. Salisbury, J.J. Craig, Articulated hands: Force control and kinematic issues, Int. J. Rob. Res. 1 (1982) 4–17.
[9] G. Cui, H. Zhang, D. Zhang, F. Xu, Analysis of the kinematic accuracy reliability of a 3-DOF parallel robot manipulator, Int. J. Adv. Rob. Syst. 12 (2015) 15.
[10] J.-P. Merlet, Jacobian, manipulability, condition number, and accuracy of parallel robots, J. Mech. Des. 128 (2006) 199–206.
[11] J. Enferadi, A.A. Tootoonchi, Accuracy and stiffness analysis of a 3-RRP spherical parallel manipulator, Robotica 29 (2011) 193–209.
[12] P. Zhang, Z. Yao, Z. Du, Global performance index system for kinematic optimization of robotic mechanism, J. Mech. Des. 136 (2014) 031001.
[13] G. Legnani, D. Tosi, I. Fassi, H. Giberti, S. Cinquemani, The "point of isotropy" and other properties of serial and parallel manipulators, Mech. Mach. Theory 45 (2010) 1407–1423.
[14] H. Lipkin, J. Duffy, Hybrid twist and wrench control for a robotic manipulator, J. Mech., Trans. Autom. Des. 110 (1988) 138–144.
[15] C.M. Gosselin, Dexterity indices for planar and spatial robotic manipulators, in: Robotics and Automation, 1990. Proceedings., 1990 IEEE International Conference on, 1990, pp. 650–655.
[16] G. Pond, J.A. Carretero, Quantitative dexterous workspace comparison of parallel manipulators, Mech. Mach. Theory 42 (2007) 1388–1400.
[17] J. Angeles, The design of isotropic manipulator architectures in the presence of redundancies, The Int. J. Rob. Res. 11 (1992) 196–201.
[18] D. Chablat, P. Wenger, S. Caro, J. Angeles, The isoconditioning loci of planar three-DOF parallel manipulators, in: ASME 2002 International Design Engineering Technical Conferences and Computers and Information in Engineering Conference, 2002, pp. 601–606.
[19] R. Kelaiaia, A. Zaatri, Multiobjective optimization of a linear Delta parallel robot, Mech. Mach. Theory 50 (2012) 159–178.
[20] M. Hosseini, H. Daniali, Weighted local conditioning index of a positioning and orienting parallel manipulator, Scientia Iranica 18 (2011) 115–120.
[21] P. Cardou, S. Bouchard, C. Gosselin, Kinematic-sensitivity indices for dimensionally nonhomogeneous jacobian matrices, IEEE Trans. Rob. 26 (2010) 166–173.
[22] J.J. Cervantes-Sánchez, J.M. Rico-Martínez, I.J. Brabata-Zamora, J.D. Orozco-Muñiz, Optimization of the translational velocity for the planar 3-RRR parallel manipulator, J. Braz. Soc. Mech. Sci. Eng. 38 (2016) 1659–1669.
[23] T. Yoshikawa, Translational and rotational manipulability of robotic manipulators, in: American Control Conference, 1990, 1990, pp. 228–233.
[24] I. Mansouri, M. Ouali, A new homogeneous manipulability measure of robot manipulators, based on power concept, Mechatron. 19 (2009) 927–944.
[25] I. Mansouri, M. Ouali, The power manipulability–A new homogeneous performance index of robot manipulators, Rob. Comput. Integr. Manuf. 27 (2011) 434–449.
[26] S. Kucuk, Z. Bingul, Comparative study of performance indices for fundamental robot manipulators, Rob. Autom. Syst. 54 (2006) 567–573.
[27] C. Gosselin, J. Angeles, A global performance index for the kinematic optimization of robotic manipulators, J. Mech. Des. 113 (1991) 220–226.
[28] G.H. Golub, C.F. Van Loan, Matrix Computations, 3, JHU Press, 2012.
[29] J. Enferadi, A.A. Tootoonchi, A novel spherical parallel manipulator: forward position problem, singularity analysis, and isotropy design, Robotica 27 (2009) 663–676.
[30] J.-P. Merlet, Parallel Robots, 128, Springer Science & Business Media, 2006.
[31] H. Mohammadi, P.J. Zsombor-murray, J. Angeles, The isotropic design of two general classes of planar parallel manipulators, J. Field Rob. 12 (1995) 795–805.
[32] O. Alba-Gomez, P. Wenger, A. Pamanes, Consistent kinetostatic indices for planar 3-DOF parallel manipulators, application to the optimal kinematic inversion, in: ASME 2005 International Design Engineering Technical Conferences and Computers and Information in Engineering Conference, 2005, pp. 765–774.
[33] J. Wu, J. Wang, T. Li, L. Wang, L. Guan, Dynamic dexterity of a planar 2-DOF parallel manipulator in a hybrid machine tool, Robotica 26 (2008) 93–98.
[34] T. Yoshikawa, Dynamic manipulability of robot manipulators, Trans. Society Instrum. Control Eng. 21 (1985) 970–975.